mTOR target NDRG1 confers MGMT-dependent resistance to alkylating chemotherapy

Weiler, M ; Blaes, J ; Pusch, S ; Sahm, F ; Czabanka, M ; Luger, S ; Bunse, L ; Solecki, G ; Eichwald, V ; Jugold, M ; Hodecker, S ; Osswald, M ; Meisner, C ; Hielscher, T ; Rübmann, P ; Pfenning, P N ; Ronellenfitsch, M ; Kempf, T ; Schnölzer, M ; Abdollahi, A ; Lang, F ; Bendszus, M ; von Deimling, A ; Winkler, F ; Weller, M ; Vajkoczy, P ; Platten, M ; Wick, W

Abstract: A hypoxic microenvironment induces resistance to alkylating agents by activating targets in the mammalian target of rapamycin (mTOR) pathway. The molecular mechanisms involved in this mTOR-mediated hypoxia-induced chemoresistance, however, are unclear. Here we identify the mTOR target N-myc downstream regulated gene 1 (NDRG1) as a key determinant of resistance toward alkylating chemotherapy, driven by hypoxia but also by therapeutic measures such as irradiation, corticosteroids, and chronic exposure to alkylating agents via distinct molecular routes involving hypoxia-inducible factor (HIF)-1alpha, p53, and the mTOR complex 2 (mTORC2)/serum glucocorticoid-induced protein kinase 1 (SGK1) pathway. Resistance toward alkylating chemotherapy but not radiotherapy was dependent on NDRG1 expression and activity. In posttreatment tumor tissue of patients with malignant gliomas, NDRG1 was induced and predictive of poor response to alkylating chemotherapy. On a molecular level, NDRG1 bound and stabilized methyltransferases, chiefly O(6)-methylguanine-DNA methyltransferase (MGMT), a key enzyme for resistance to alkylating agents in glioblastoma patients. In patients with glioblastoma, MGMT promoter methylation in tumor tissue was not more predictive for response to alkylating chemotherapy in patients who received concomitant corticosteroids.

DOI: https://doi.org/10.1073/pnas.1314469111

BIOLOGICAL SCIENCES: Medical Sciences

The mTOR target NDRG1 confers MGMT-dependent resistance to alkylating chemotherapy

Markus Weiler[1,2,8,17], Jonas Blaes[1,2,17], Stefan Pusch[1,3,10,17], Felix Sahm[1,3,10], Marcus Czabanka[11], Sebastian Luger[1,2,8], Lukas Bunse[1,5,8], Gergely Solecki[1,2], Viktoria Eichwald[1,7], Manfred Jugold[1,7], Sibylle C. Hodecker[1,2,8], Matthias Osswald[1,2,8], Christoph Meisner[13], Thomas Hielscher[1,6], Petra Rübmann[1,7], Philipp-Niclas Pfenning[1,2], Michael Ronellenfitsch[15], Tore Kempf[4], Martina Schnölzer[4], Amir Abdollahi[1,9], Florian Lang[14], Martin Bendszus[10], Andreas von Deimling[1,3,11], Frank Winkler[1,2,8], Michael Weller[16], Peter Vajkoczy[12], Michael Platten[1,5,8] and Wolfgang Wick[1,2,8,18]

[1]German Cancer Consortium (DKTK), Clinical Cooperation Units [2]Neurooncology and [3]Neuropathology, [4]Functional Proteome Analysis, [5]Helmholtz Group Experimental Neuroimmunology [6]Biostatistics, and [7]Small Animal Imaging Facility, German Cancer Research Center (DKFZ), INF 280, D-69120 Heidelberg; Departments of [8]Neurooncology and [9]Radiation Oncology at the National Center for Tumor Diseases, Departments of [10]Neuroradiology and [11]Neuropathology, University Hospital Heidelberg, INF 400, D-69120 Heidelberg; [12]Neurosurgery Clinic Charité, University Medicine Berlin, Augustenburger Platz 1, D-13353 Berlin; [13]Department of Medical Biometry and [14]Physiology, Geissweg 3, D-72076 Tübingen, University of Tübingen; [15]Dr. Senckenberg Institute of Neurooncology, Goethe-University Hospital Frankfurt, Schleusenweg 2-16, D-60528 Frankfurt am Main; all Germany; [16]Department of Neurology, Frauenklinikstrasse 26, CH-8090 Zurich, University Hospital Zurich, Switzerland

[17]These authors contributed equally to this work

[18]Correspondence: Wolfgang Wick, MD, Department of Neurooncology, Neurology Clinic and National Center for Tumor Diseases, University Hospital Heidelberg, Im Neuenheimer Feld 400, D-69120

Heidelberg, Germany; phone: +49-6221-56-7075; fax: +49-6221-56-7554; email: wolfgang.wick@med.uni-heidelberg.de.

Running Title: Resistance to alkylating chemotherapy by NDRG1

Conflict of interest: None.

Keywords: MGMT; mTORC2; NDRG1; resistance; SGK1; steroids

ABSTRACT

A hypoxic microenvironment induces resistance to alkylating agents by activating targets in the mammalian target of rapamycin (mTOR) pathway. The molecular mechanisms involved in this mTOR-mediated hypoxia-induced chemoresistance, however, are unclear. Here we identify the mTOR target N-myc downstream regulated gene (NDRG)1 as a key determinant of resistance towards alkylating chemotherapy, driven by hypoxia but also therapeutic measures such as irradiation, corticosteroids and chronic exposure to alkylating agents *via* distinct molecular routes involving hypoxia-inducible factor (HIF)1alpha, p53 and the mTOR complex (mTORC)2/serum glucocorticoid-induced protein kinase (SGK)1 pathway. Resistance towards alkylating chemotherapy but not radiotherapy was dependent on NDRG1 expression and activity. In post-treatment tumor tissue of patients with malignant gliomas NDRG1 was induced and predictive of poor response to alkylating chemotherapy. On a molecular level NDRG1 bound and stabilized methyltransferases, chiefly O^6-methylguanine-DNA methyltransferase (MGMT), a key enzyme for resistance to alkylating agents in glioblastoma patients. Importantly, in patients with glioblastoma, *MGMT* promoter methylation in tumor tissue was not predictive for response to alkylating chemotherapy anymore in patients who were previously treated with radiotherapy or who received concomitant corticosteroids.

Statement of significance

NDRG1 is a central and druggable molecular hub integrating diverse therapy-induced microenvironmental factors to promote resistance towards alkylating chemotherapy and suggest that NDRG1-mediated chemoprotection is achieved *via* binding and stabilizing methyltransferases, such as MGMT.

\body

INTRODUCTION

Primary or acquired antitumor therapy resistance is one of the major obstacles in oncology. For glioma, to date this is pivotal for the standard of care, radiotherapy and temozolomide (TMZ) alkylating chemotherapy. The DNA repair protein O^6-methylguanine-DNA methyltransferase (MGMT) plays a critical role in primary resistance to alkylating agents (1,2). How microenvironmental factors or co-treatments influence acquired resistance to alkylating chemotherapy, however, is incompletely understoood. Serving as a central signaling hub integrating multiple intra- and extracellular cues, the 289-kDa serine/threonine kinase mammalian target of rapamycin (mTOR) is an attractive anticancer target. Activation of the signaling network engaged by the protein inositol-3 kinase/AKT/mTOR axis frequently occurs by activation of receptor tyrosine kinases (RTK), chiefly the epidermal growth factor receptor (EGFR) being the most commonly altered RTK in glioblastomas. However, mere inhibition of EGFR or mTOR has been ineffective in glioblastomas.

The hypoxic microenvironment has been proposed to serve as germ center for more aggressive and therapy-resistant tumor cell phenotypes (3) especially preventing the efficacy of radiotherapy (4,5). Hypoxia induces resistance to several anticancer agents in neurons (6), but also glioma cells (7). Molecular mechanisms for hypoxia-mediated chemoresistance in glioma are only poorly understood. In general, hypoxia causes the accumulation of the transcription factor hypoxia-inducible factor 1 (HIF-1) leading to the expression of hypoxia-inducible genes such as those for *vascular endothelial growth factor* (*VEGF*) and *N-myc downstream regulated gene* (*NDRG*)*1* (8). The NDRG family of proteins consists of four evolutionary conserved members, NDRG1-4. The first member to be discovered and responsible for the family name was NDRG1, because its expression is repressed by the proto-oncogenes MYCN and MYC. However, regulation or the precise molecular and cellular functions of these family members have not been fully elucidated (9). It has been hypothesized that NDRG1 expression is inversely correlated with survival in glioblastomas

(10), but the molecular and functional mechanisms involved in this association remain unclear.

To identify critical pathways involved in the chemoresistance of gliomas evoked by microenvironmental factors, particularly hypoxia, we initiated an unbiased proteomics approach.

MATERIALS AND METHODS

Cell culture, reagents, transfections and treatment regimens

Details are provided in the Supplementary Methods.

Plasmid-based knock-down of *NDRG1*

To silence *NDRG1* gene expression, two short-hairpin RNA (shRNA) sequences targeting different sites were cloned into the pSUPER-puro vector (11). The sequences are provided in the Supplementary Methods.

Lentiviral preparations

Lentiviral particles for the knock-down experiments were produced by co-transfecting psPAX2, pMD2.G (both Addgene plasmid 12259) and pLKO.1 constructs (TRC1, Sigma-Aldrich) in HEK293T cells using TransIT LT1 (Mirus Bio, Madison, WI, USA). Details are given in the Supplementary Methods.

Quantitative reverse transcription polymerase chain reaction

Quantitative Reverse Transcription Polymerase Chain Reaction (qRT-PCR) was done as described (12). *NDRG1-4 and SGK1* expression results were normalized to *glyceraldehyde-3-phosphate dehydrogenase* (*GAPDH*). Primer sequences are given in Table S6.

Cloning of NDRG1 variants

NDRG1 dephospho-variants were generated by using site-directed mutagenesis PCR and changing the codons of the phospho-sites Thr and Ser to Val and Ala, respectively. Two different phosphorylation-deficient variants NDRG1-T346V-T356V and NDRG1-T328V-S330A-T346V-T356V were generated.

Immunoblot

Preparation of cell lysates and immunoblots were performed as described before (13). Antibodies are given in Table S8.

Proximity Ligation Assay (PLA)

T98G and LN-229 cells (n = $2x10^4$) were confluently grown at O_2 of 1% on cover slips for 72 h. Fixation was done using 30 min Cytofixx Pump Spray cell path and 30 min 4% PFA. For detection the Red Duolink *In Situ* PLA Kit was performed according to manufacturer´s instructions with anti-NDRG1 polyclonal rabbit (Sigma-Aldrich) and mouse anti-MGMT (Life Technologies, Carlsbad, CA, USA) applied for 12 h. Mounting was done with VECTASHIELD HardSet Mounting Medium with DAPI.

Animal experiments, image processing and histology

All animal work was approved by the governmental authorities (Regierungspräsidium Karlsruhe, Germany) and supervised by institutional animal protection officials in accordance with the NIH guidelines 'Guide for the Care and Use of Laboratory Animals'. Details are provided in the Supplement.

Clinical data

All clinically-related research in this manuscript is covered by the Ethical Vote for the UKT-05 (14), NOA-04 (15) and NOA-08 (16) trials.

Statistical analysis

Quantitative *in vitro* data are expressed as mean ± standard deviation (SD), as indicated. All *in vitro* experiments reported here represent at least three independent replications performed in triplicate if not otherwise stated. Statistical significance was assessed by two-sided Student's t-Test or ANOVA (Excel, Microsoft, Seattle, WA, USA). Values of $p < 0.05$ were considered significant and asterisked without correction for multiple statistical tests. Mouse glioma volumes were corrected for outliers using Grubbs' test. Survival data were

plotted by the Kaplan-Meier method and analyzed by the log-rank test. SigmaPlot Software was used for all analyses.

RESULTS

Hypoxia-induced alkylator but not radiotherapy resistance in malignant gliomas depends on NDRG1

To identify factors that mediate hypoxia-induced alkylator resistance (Fig. S1a), we screened human glioma cell lines for their response to alkylating chemotherapy in hypoxic conditions and subjected LN-229 glioma cells to a proteome screen (Fig. S1b). This screen revealed hypoxia-specific upregulation of seven and downregulation of two proteins (Table S1), of which upregulated NDRG1 was further analyzed since (i) its upregulation in hypoxia was unequivocally confirmed in all conducted assays (Table S1), (ii) it had been implicated as a target of hypoxia (17) and a prognostic factor in various types of tumors (18,19) and (iii) it was found down-regulated in a transcriptome analysis following pharmaceutical mTOR inhibition with RAD001 (at http://www.ebi.ac.uk/arrayexpress under the accession number: E-MEXP-3802). Hypoxia induced NDRG1 in all tested glioma cell lines (Fig. 1a). This was specific for NDRG1, as NDRG2-4 were not differentially regulated (Fig. 1b). In human glioma specimens, NDRG1 was associated with the degree of malignancy, and in glioblastomas prominently expressed in putatively hypoxic, perinecrotic areas (Fig. 1c, Fig. S2a).

Knock-down of *NDRG1* resulted in sensitization of established glioma cells and naturally NDRG1-high expressing T269 and T325 primary glioma cells to TMZ (Fig. 1d upper panels, Fig. S3a), indicating that NDRG1 mediates hypoxia-induced resistance to alkylating agents. Conversely, NDRG1-overexpressing cells showed a reduction in the TMZ-induced G2/M arrest (Fig. 1d lower panels, Figure S3b), which corresponded to a reduction in proliferation *in vitro* (Fig. 1e) and tumor growth *in vivo* (Fig. 1f), while proliferation or clonogenicity of glioma cells exposed to radiotherapy at 2 or 4 Gy remained unaffected (Fig. S3d). Of note, NDRG1 overexpressing cells not exposed to TMZ proliferated slower than the controls (Fig. 1e, Fig. S4d,f).

NDRG1 is transcriptionally activated by radiotherapy and phosphorylated in the course of TMZ treatment

Next, we analysed the influence of therapeutic measures altering the tumor microenvironment on NDRG1 expression and activity. *In vitro*, irradiation (Fig. S5a) but not TMZ induced NDRG1 mRNA and protein expression. In contrast to hypoxia, irradiation-induced NDRG1 expression was dependent on p53 expression (Fig. S5b, Fig. S4a and b), but was not impaired by *HIF-1*α or *HIF-2*α gene silencing (Fig. S5c), indicating that hypoxia and irradiation employ diverse signalling pathways to induce chemoresistance *via* NDRG1. Interestingly, long-term exposure to TMZ led to an increased phosphorylation of NDRG1 at position T346 in surviving cells (Fig. S5d). NDRG1 phosphorylation at T346 is associated with increased activity (20). Collectively, these data indicate that hypoxia and irradiation but not alkylating chemotherapy activate NDRG1 *via* distinct pathways resulting in resistance towards alkylating chemotherapy (Fig. S6).

NDRG1 is a predictive marker for response to alkylating chemotherapy

Next we interrogated patient tumor tissue to recapitulate the relevance of inducible NDRG1 for therapy resistance. NDRG1 is induced at tumor recurrence (Fig. 2a, Fig. S2b). Interestingly, as opposed to tumor tissue at diagnosis, NDRG1 expression in the treated tissues was not predominantly seen in perinecrotic areas anymore, but NDRG1 was widely expressed in glioblastoma cells even perivascularly opposed to the situation in the untreated tumors (Fig. 2b). NDRG1 expression in patients with low-grade gliomas progressing without interim genotoxic treatment also increased (Fig. S2b). High NDRG1 levels at recurrence predicted poor response to alkylating chemotherapy, but not to the antiangiogenic agent bevacizumab, another frequent non-alkylating therapeutic measure in glioma therapy, in a small group of patients (Table S2). A predictive role of NDRG1 for poor response to radiochemotherapy was suggested by *post hoc* NDRG1 expression analyses, which revealed that progression-free survival (PFS) and overall survival (OS) of glioblastoma patients from the UKT-05 trial (14) with moderate or high expression of NDRG1 was reduced

compared to patients with low NDRG1-expressing tumors (Fig. 2c). This was supported by an analysis of the REpository for Molecular BRAin Neoplasia DaTa (REMBRANDT) database, which revealed that the OS of glioblastoma patients with intratumoral upregulation of *NDRG1* was reduced compared to patients with intermediate or downregulated expression of the *NDRG1* transcript (Fig. 2d). To determine whether the prognostic impact of NDRG1 is specifically related to alkylating chemotherapy, tissue samples of the NOA-04 trial comparing primary radiotherapy with primary alkylating chemotherapy (15) were analyzed. NDRG1 expression was associated with reduced PFS in TMZ treated patients, but not with radiotherapy in this not preplanned subgroup analysis (Fig. 2e). Collectively, these data from several study patient populations suggest that NDRG1 expression in glioma tissue is associated with a poor response specifically to alkylating chemotherapy.

NDRG1 is an effector of the mTORC2/SGK1 pathway

As opposed to transcriptional regulation of *NDRG1* by hypoxia and radiation, the signaling cascade that mediates NDRG1 phosphorylation at the T346 residue in TMZ-resistant glioma cells is unclear, but most likely downstream of mTOR. Knock-down of the *mTORC2* subunit *rapamycin-insensitive companion of mTOR* (*RICTOR*) but not the *mTORC1 subunit regulatory associated protein of mTOR* (*RAPTOR*) resulted in a reduction of NDRG1 phosphorylation and expression (Fig. 3a, upper and middle panel). Control of NDRG1 phosphorylation by RICTOR is independent of its transcriptional regulation of NDRG1 as knock-down of *RICTOR* in cells with exogenous NDRG1 expression, resulted in a reduction of NDRG1 phosphorylation and subsequent sensitization towards TMZ (Fig. 3a, lower panel).

Studies in pancreatic cancer indicated that phosphorylation of NDRG1 at this specific site is mediated by the putative mTOR downstream effector, serum glucocorticoid-induced protein kinase (SGK)1 (21). Dexamethasone (DEX), which is an integral part in the treatment of malignant gliomas as a means to control edema (22), induced *SGK1* transcription and increased the phosphorylation of NDRG1 at T346 (Fig. 3b). To test the hypothesis that

treatment with DEX blunts the efficacy of alkylating chemotherapy in patients with glioblastoma, we performed a subgroup analysis of the NOA-08 trial. In this trial elderly patients with malignant astrocytoma received radiotherapy or TMZ until progression and were treated with steroids at clinical discretion to treat or prevent vasogenic cerebral edema (23). Subgroup analyses allowed to generate the hypothesis that steroid administration was associated with reduced PFS of patients treated with TMZ but not radiotherapy (Fig. 3c, Table S3). An animal experiment with U87MG cells supports a negative impact of DEX on the efficacy of TMZ (Fig. 3d and Fig. S6b). Pharmacological inhibition of SGK1 by EMD638683 resulted in decreased phosphorylation of T346 and overcame the NDRG1-mediated protection from TMZ (Fig. 3e). Importantly, this is neither specific for TMZ nor for glioma cells as EMD638683 treatment also decreased constitutive NDRG1 phosphorylation in pancreatic, breast, colon and ovarian cancer cells (Fig. S7a). EMD638683-mediated sensitization towards chemotherapy was specific for alkylating agents as a sensitization was seen for lomustine in breast and ovarian cell lines (Fig. S7b), but resistance neither to 5-fluorouracil nor to cisplatin was decreased (Fig. S7c,d).

NDRG1 interacts with three DNA repair enzymes and promotes protein stability/activity of MGMT

Although described for the mediation of cisplatin resistance in glioma *via* activation of the mTORC2-mediated cascade, in the present paradigm, nuclear factor (NF)κB is not influenced by the NDRG status (Fig. S8c). To unravel the molecular mechanisms, by which NDRG1 prevents TMZ-induced cytotoxicity, a yeast two-hybrid screen for potential interaction partners was performed. Of 119 possible interaction partners (Table S4), three proteins were involved in DNA repair: polynucleotide 3′-phosphatase, polynucleotide 5′-hydroxyl-kinase (PNKP), DNA-(apurinic or apyrimidinic site) lyase (APEX1) and MGMT (Fig. 4a). Interaction of these three proteins with NDRG1 was verified in a pull-down assay using HEK293 cells (Fig. 4b). The interaction of MGMT and NDRG1 was studied further as (i) particularly MGMT has been implicated in mediating the resistance of gliomas to alkylating

agents (23,24), (ii) only MGMT expression correlated with TMZ resistance in gliomas cells, and (iii) knock-down of *MGMT* but not *PNKP* or *APEX1* rendered glioma cells more susceptible towards the antiproliferative effects of TMZ (Fig. 4c,d). Bimolecular fluorescence complementation (BiFC) assays confirmed a direct interaction of MGMT and NDRG1 both in HEK293T (Fig. 5e, upper panel) and T98G glioma cells (Fig. S10a) exogenously overexpressing the two proteins. Importantly, proximity ligation assays (PLA) also revealed this interaction for native T98G cells exposed to hypoxia in the nucleus (Fig. 4e, lower panel). This interaction critically depended on SGK1 activity (Fig. S11) and phospho-threonine or -serine SGK1 target sites in the C-terminus of NDRG1 since mutation of T328, 330, 346 and 356 significantly reduced the NDRG1/MGMT interaction in BiFC assays (Fig. 4f). Importantly, forced expression of NDRG1 did not render cells resistant to TMZ when *MGMT* was knocked down, indicating that TMZ resistance mediated by NDRG1 is dependent on MGMT (Fig. 4d). Next, the hypothesis was tested that NDRG1 increases MGMT activity resulting in enhanced repair of DNA damage mediated by alkylating agents. Exogenous expression of NDRG1 resulted in augmented MGMT levels at 8 hours (Fig. 5a, upper panel) when RNA synthesis was blocked. Exposure of these cells to TMZ resulted in an expected decrease *via* depletion of MGMT expression at 4 hours independent from NDRG1 but a faster recovery of MGMT in NDRG1 overexpressing cells (Fig. 5a, lower panel). Indeed, exogenous expression of NDRG1 resulted in enhanced demethylation activity of MGMT in gliomas cells exposed to TMZ (-0.25, 95%CI (-0.41 - -0.09), p=0.0219) (Fig. 5b). To test whether this is relevant for treatment outcome in patients with glioblastoma we again performed *post hoc* subgroup analyses of the NOA-08 trial. Stratification of the TMZ-treated group of NOA-08 despite all limitations of this approach revealed that steroid administration resulted in a reduced PFS only in patients with a methylated *MGMT* promoter and hence inactive MGMT (Fig. 5c, Table S5), suggesting that treatment of patients with DEX by inducing NDRG1 activity compromises the efficacy of alkylating chemotherapy independent of DNA repair activity, although there may be confounding factors triggering a decision for or against DEX treatment. In addition, also in patients who failed radiotherapy in

this trial and who received salvage chemotherapy with TMZ (Table S5), MGMT activity was not predictive of response to chemotherapy anymore as opposed to the primary situation (Fig. 5c). Collectively these data indicate that multiple treatment measures including treatment with steroids and radiotherapy by inducing NDRG1 can impair inherent susceptibility of *MGMT*-methylated glioma cells to the therapeutic effects of alkylating chemotherapy (Fig. 5d).

DISCUSSION

Hypoxia-induced resistance (Fig. S1a) is implicated in treatment resistance not only to radio- but also chemotherapy (5). We identified NDRG1 as a novel clinically relevant resistance factor induced by both hypoxia and iatrogenic stimuli such as irradiation and corticosteroids. In line with this, we found NDRG1 expression in gliomas, which increased with malignancy (Fig. 1c), in untreated tumors mostly restricted to the perinecrotic, hypoxic areas (Fig. 1c), whereas in the recurrent tumors, subjected to treatment with irradiation, chemotherapy and steroids, NDRG1 was not only further upregulated, but also expressed in the tumor bulk and in perivascular regions (Fig. 2a,b, Figure S2a), although some induction of NDRG1 with progression is also observed without genotoxic treatment (Figure S2b). These data do not support the previously proposed proapoptotic function of NDRG1 in gliomas (17), but rather lay the first hint that NDRG1 can play a pivotal role in therapy resistance.

Several analyses of tumor tissue specimens from clinical studies of malignant gliomas support the notion that NDRG1 is induced by radiochemotherapy with TMZ (Fig. 2a) and, more importantly, renders gliomas insensitive to chemotherapy with alkylating chemotherapy (Fig. 2c-e, Table S2). *In vitro* studies did not suggest a propensity of alkylating chemotherapy to induce NDRG1 expression (Fig. S5d), whereas irradiation appeared to be a strong inducer of NDRG1 (Fig. S5a). Another explanation for the increased expression of NDRG1 *post* therapy might be the cytoprotective effect of NDRG1 providing an advantage for NDRG1-expressing cells during treatment with TMZ (Fig. 1d-f), but not radiotherapy (Fig. S3c) or induction with the tumor progression (Fig. S2b).

An alternative mechanism of NDRG1 activation is phosphorylation at T346, which is increased in TMZ-resistant cell lines (Fig. S8c). Phosphorylation of NDRG1 at T346 is triggered by SGK1 (21), an mTORC2 target. Tanaka et al. recently demonstrated that EGFRvIII-activated mTORC2 is relevant in the mediation of resistance towards cisplatin in glioblastoma. They used pNDRG1 as a marker for pathway activity (25). We demonstrate that the mTORC2 complex regulated NDRG1 not only on a posttranslational level through

SGK1 but also transcriptionally (Fig. 3a, middle panel). In addition to mTORC1, which increases HIF-1α-levels in normoxic conditions by stimulating the cap-dependent translation from the 5′-untranslated region of the *HIF-1α* mRNA (26), mTORC2 has been implicated in the regulation of HIF (27).

Pharmacological inhibition of the mTORC2 target SGK1 by EMD638683 overcame the NDRG1-mediated protection from TMZ (Fig. 3d). SGK1 has been shown to promote cell survival and cell-cycle progression in a multitude of human tumors. Since the *SGK1* promoter contains a glucocorticoid response element and SGK1 is well-known to be inducible by dexamethasone treatment in different tumors (28,29), we were not surprised to find SGK1 induced by dexamethasone in glioblastoma cells as well. This transcriptional activation of *SGK1* was accompanied by an increased phosphorylation of NDRG1 at T346 (Fig. 3b). The clinical relevance of this finding is underscored by both the frequent use of dexamethasone in glioma to treat vasogenic edema and by the interesting effect of dexamethasone treatment in the NOA-08 cohort of TMZ-treated patients with intratumoral *MGMT* promoter methylation, who should derive the largest benefit from the alkylating chemotherapy. In these patients, co-treatment with steroids halved the PFS compared with TMZ treatment without steroid administration (Fig. 5c, Table S5). One alternative contributing factor is that larger tumors, which may require higher steroid doses, are more difficult to control. Further, patients with inactive MGMT would also suffer most from blood-brain-barrier normalizing effects of corticosteroids (30).

Importantly, resistance mediated by NDRG1 was neither limited to gliomas nor to TMZ specifically (Fig. S7a,b and Fig. S8), but was specific for alkylating chemotherapy as the effect of radiotherapy was not influenced by NDRG1, neither in preclinical models (Fig. S3c) nor in patients with malignant gliomas (Fig. 2e). At recurrence of glioblastoma, predominantly alkylating chemotherapy was negatively impacted (Table S2).

Our interpretation of the data led us to propose an interaction of NDRG1 with factors involved in the execution or prevention of DNA damage. In our yeast-two hybrid screen, we see a protein interaction of NDRG1 the DNA repair enzymes APEX1, PNKP and MGMT

(2,31,32) (Fig. 4a,b). In line with the observation that only the expression of MGMT correlated with TMZ resistance (Fig. S8a) (33), the interaction of NDRG1 with MGMT, but not with PNKP or APEX1, proved to be of functional relevance for the resistance phenotype in malignant glioma (Fig. 4c,d). In other tumor types the interaction of NDRG1 with PNKP and/or APEX1 may be functionally relevant for the resistance phenotype. Considering the observed augmentation of MGMT levels under stress conditions in the presence of high NDRG1 levels (Fig. 5a) and the co-localization at subcellular levels (Fig. 4e), it is conceivable that NDRG1 stabilizes MGMT *via* a direct protein-protein interaction, thus fulfilling a chaperone-like function. Nevertheless, MGMT alone cannot account for the observed NDRG1-dependent resistance phenotype, since MGMT-negative U87MG cells also become more resistant upon an elevated NDRG1 expression level (Fig. 1d). Patients with intratumoral methylation of the *MGMT* promoter and thus putatively no MGMT expression become more resistant in response to steroid treatment (Table S4, Figure 5c). These data suggest that there may be additional mechanisms involved in the NDRG1-provoked resistance to alkylating chemotherapy in gliomas.

In conclusion, we identified NDRG1 as a novel hypoxia-, steroid- and mTORC2/SGK1-regulated molecule in glioma that may be developed as a predictive biomarker for response to treatment with TMZ in high-grade gliomas. Its TMZ-protective effect makes NDRG1 an attractive candidate for targeted therapy not only in gliomas but also a variety of other cancer types, potentially *via* inhibition of SGK1. The preclinical data suggest multiple levels of cell-intrinsic (mTORC1), microenvironmental (hypoxia) and iatrogenic (radiotherapy, dexamethasone) influences on this critical signaling pathway downstream of several growth factor receptors (34). The mTORC2/SGK1/NDRG1 pathway may serve as targets for future preclinical and clinical research on therapy resistance (Fig. 5d).

SUPPLEMENTAL INFORMATION

Supplemental Information includes figures, tables, experimental procedures, and references.

ACKNOWLEDGMENTS

We thank Torsten Schmenger for excellent technical assistance, Mona Friedrich, BSc for help with the lentiviral transfections and animal experiments as well as Hans-Werner Pledl for the supply with TMZ-resistant LN-18 sublines. The *HIF*-knock-down cell lines were kindly provided by Prof. Dr. Till Acker, Giessen, Germany. EMD 638683 was kindly provided by Dr. Thomas Fuchss, Merck KGaA, Merck Serono, Darmstadt, Germany. Support by the DKFZ Light Microscopy Facility is gratefully acknowledged. This work was supported within the Brain Tumor Network (BTNplus; Subproject 6) of the National Genome Research Network (NGFNplus) by the Federal Ministry of Education and Research (BMBF), the 'Förderverein für Gehirntumorforschung Karlsruhe e.V.', the Charitable Hertie Foundation and the Deutsche Forschungsgemeinschaft (SFB 773 and SFB 938 TP K). J.B. is a doctoral student in the PhD Program of the DKFZ.

REFERENCES

1. Sarkaria JN, *et al.* (2008) Mechanisms of chemoresistance to alkylating agents in malignant glioma. *Clin Cancer Res* 14:2900-2908.
2. Dunn GP, *et al.* (2012) Emerging insights into the molecular and cellular basis of glioblastoma. *Genes Dev* 26:756-784.
3. Amberger-Murphy V (2009) Hypoxia helps glioma to fight therapy. *Curr Cancer Drug Targets* 9:381-390.
4. Harris AL (2002) Hypoxia: a key regulatory factor in tumor growth. *Nat Rev Cancer* 2:38-47.
5. Winkler F, *et al.* (2004) Kinetics of vascular normalization by VEGFR2 blockade governs brain tumor response to radiation: role of oxygenation, angiopoietin-1, and matrix metalloproteinases. *Cancer Cell* 6:553-563.
6. Wick A, *et al.* (2002) Hypoxic neuroprotection requires sequential activation of vascular endothelial growth factor receptor and Akt. *J Neurosci* 22:6401-6407.
7. Henze AT, *et al*. (2010) Prolyl hydroxylases 2 and 3 act in gliomas as protective negative feedback regulators of hypoxia-inducible factors. *Cancer Res* 70:357-366.
8. Salnikow K, Blagosklonny MV, Ryan H, Johnson R, & Costa M (2000) Carcinogenic nickel induces genes involved with hypoxic stress. *Cancer Res* 60:38-41.
9. Melotte V, *et al.* (2010) The N-myc downstream regulated gene (NDRG) family: diverse functions, multiple applications. *FASEB J* 24:4153-4166.
10. Sun B, *et al.* (2009) Decreased expression of NDRG1 in glioma is related to tumor progression and survival of patients. *J Neurooncol* 94:213-219.
11. Brummelkamp TR, Bernards R, & Agami R (2002) Stable suppression of tumorigenicity by virus-mediated RNA interference. *Cancer Cell* 2:243-247.
12. Opitz CA et al. An endogenous ligand of the human aryl hydrocarbon receptor promotes tumor formation. Nature. 2011;478:197-203.
13. Weiler M, *et al*. (2013) Suppression of proinvasive RGS4 by mTOR inhibition optimizes glioma treatment. *Oncogene* 32:1099-1109.
14. Weiler M, *et al.* (2010) Phase II trial of radiochemotherapy with daily concomitant and adjuvant intensified (one week on / one week off) TMZ plus indomethacin in newly diagnosed glioblastoma: UKT-05. *Int J Rad Biol Phys* 77:670-676.

15. Wick W, *et al*. (2009) NOA-04 randomized phase III trial of sequential radiochemotherapy of anaplastic glioma with PCV or TMZ. *J Clin Oncol* 27:5874-5880.
16. Wick W, *et al*. (2012) TMZ chemotherapy alone versus radiotherapy alone for malignant glioma in the elderly: the NOA-08 randomised, phase 3 trial. *Lancet Oncol* 13:707-715.
17. Zhang P, Tchou-Wong KM, & Costa M (2009) Egr-1 mediates hypoxia-inducible transcription of the NDRG1 gene through an overlapping Egr-1/Sp1 binding site in the promoter. *Cancer Res* 67:9125-9133.
18. Azuma K, *et al.* (2012) NDRG1/Cap43/Drg-1 may Predict tumor angiogenesis and poor outcome in patients with lung cancer. *J Thorac Oncol* 7:779-789.
19. Zhang SB, Song SP, Li B, Zhou YS, & Zhang YD (2011) Expression of N-myc downstream-regulated gene 1 in primary gallbladder carcinoma and its correlation with clinicopathological features and clinical outcome. *Med Oncol* Jul 7, EPub.
20. Garcia-Martinez JM, & Alessi DR (2008) mTOR complex 2 (mTORC2) controls hydrophobic motif phosphorylation and activation of serum- and glucocorticoid-induced protein kinase 1 (SGK1). *Biochem J* 416:375-385.
21. Murakami Y, *et al*. (2010) Identification of sites subjected to serine/threonine phosphorylation by SGK1 affecting N-myc downstream-regulated gene 1 (NDRG1)/Cap43-dependent suppression of angiogenic CXC chemokine expression in human pancreatic cancer cells. *Biochem Biophys Res Commun* 396:376-381.
22. Jones TS, & Holland EC (2012) Standard of care therapy for malignant glioma and its effect on tumor and stromal cells. *Oncogene* 31:1995-2006.
24. Hegi ME, *et al*. (2005) MGMT gene silencing and benefit from TMZ in glioblastoma. *N Engl J Med* 352:997-1003.
25. Tanaka K, *et al*. (2011) Oncogenic EGFR signaling activates an mTORC2-NF-kappaB pathway that promotes chemotherapy resistance. *Cancer Discov* 1:524-538.
26. Laughner E, Taghavi P, Chiles K, Mahon PC, & Semenza GL (2001) HER2 (neu) signaling increases the rate of hypoxia-inducible factor 1alpha (HIF-1alpha) synthesis: novel mechanism for HIF-1-mediated vascular endothelial growth factor expression. *Mol Cell Biol* 21:3995-4004.
27. Toschi A, Lee E, Gadir N, Ohh M, & Foster DA (2008) Differential dependence of hypoxia-inducible factors 1 alpha and 2 alpha on mTORC1 and mTORC2. *J Biol Chem* 283:34495-34499.

28. Maiyar AC, Phu PT, Huang AJ, & Firestone GL (1997) Repression of glucocorticoid receptor transactivation and DNA binding of a glucocorticoid response element within the serum/glucocorticoid-inducible protein kinase (sgk) gene promoter by the p53 tumor suppressor protein. Mol Endocrinol 11:312-329.
29. Mikosz CA, *et al*. (2001) Glucocorticoid receptor-mediated protection from apoptosis is associated with induction of the serine/threonine survival kinase gene, sgk-1. *J Biol Chem* 276:16649-16644.
30. Weller M, Schmidt C, Roth W, & Dichgans J. (1997) Chemotherapy of human malignant glioma: prevention of efficacy by dexamethasone? *Neurology* 48:1704-1709.
31. Freschauf GK, et al. (2009) Identification of a small molecule inhibitor of the human DNA repair enzyme polynucleotide kinase/phosphatase. *Cancer Res* 69:7739-7746.
32. Kaina B, Christmann M, Naumann S, & Roos WP (2009) MGMT: key node in the battle against genotoxicity, carcinogenicity and apoptosis induced by alkylating agents. *DNA Repair (Amst)* 6:1079-1099.
33. Hermisson M, *et al*. (2006) MGMT and p53 status predict TMZ sensitivity in human malignant glioma cells. *J Neurochem* 96:766-776.
34. Stommel JM, *et al*. (2007) Coactivation of receptor tyrosine kinases affects the responses of tumor cells to targeted therapies. *Science* 318:287-290.

FIGURE LEGENDS

Figure 1: NDRG1 is a hypoxia-associated chemoresistance marker in glioma

(a) Immunoblot analyses for NDRG1 of lysates prepared from glioma cells exposed to 1% O_2 (H) or 21% O_2 (N) for the indicated intervals. α-tubulin served as a loading control. (b) qRT-PCR analysis of *NDRG* isoforms exposed to 1% O_2 (mean ± SD, $n = 3$, $^{**}p < 0.01$, $^{***}p < 0.005$). (c) NDRG1 staining in WHO °II ($n = 46$), WHO °III ($n = 57$) and WHO °IV ($n = 81$) gliomas presented as number of NDRG1+ cells per field (mean ± SD). Representative images of scattered NDRG1+ cells (left panels), increased numbers of NDRG1+ cells (middle panels) and perinecrotic NDRG1+ cells are depicted by the specific red staining. (d) Cell cycle distributions and mean G2/M-arrest of TMZ-treated glioma cells relative to DMSO-(vehicle-) treated cells dependent on the NDRG1 status. TMZ concentrations used were U87MG – 10 µM, T269 – 40 µM, T325 – 300 µM, T98G – 300 µM and the medium was changed every 24 h with addition of fresh TMZ. Upper panel: Lentiviral knock-down in U87MG, T269 and T325 GIC. Lower panel: NDRG1 overexpression in U87MG and T98G cells. (e) Proliferation of TMZ/vehicle-treated U87MG cells overexpressing NDRG1 or control in RTCA. (f) MRI-determined tumor volumes of intracranially implanted U87MG gliomas overexpressing NDRG1 or control vector. TMZ was given (blue arrow) as described in Material and Methods ($^{*}p < 0.05$ *versus* control, t-test, $n = 6$).

Figure 2: NDRG1 is induced by glioblastoma therapy and serves as a negative prognostic factor

(a) Representative tissues of 19 patients prior to and at recurrence after radiochemotherapy with TMZ were scored for the number of NDRG1-positive cells (mean ± SD). (b) Representative perivascular tumor region from 20 relapsed (after radiochemotherapy) glioblastoma tissue samples. (c) Correlation of NDRG1 levels and PFS (upper plot) or OS (lower plot) of glioblastoma patients of the UKT-05 trial. (d) NDRG1 expression relative to

patient survival in glioblastoma (REMBRANDT). (e) Correlation of NDRG1 levels and PFS of patients with anaplastic gliomas of the NOA-04 trial separated for treatment.

Figure 3: mTORC2 is a master regulator of NDRG1

(a) Immunoblot of si*RNA*-treated U87MG cells targeting *RAPTOR* or *RICTOR* (upper panel). Assessment of NDRG1 phosphorylation at T346 in si*RICTOR* transfected U87MG_LV-NDRG1 cells (left lower panel) and ΔG2/M after treatment with TMZ (right lower panel). *NDRG1* mRNA expression 48 h after si*RNA*-mediated knock-down of *RICTOR* in U87MG and T98G cells (middle panel). (b) *SGK1* mRNA expression relative to *GAPDH* in T98G 72 h after treatment with dexamethasone (DEX, left panel) and phosphorylation status of NDRG1 24 to 72 h after DEX treatment (right panel). (c) Progression-free survival of the NOA-08 cohort patients differentiated according to treatment (radiotherapy (RT) *versus* TMZ) and steroid use. (d) Upper panel: Timeline depicting course of animal experiment including dates of MRI-measurements and treatment period. Lower panel: Tumor volumes on postoperative day 24. Left segment: Comparison of mean tumor volumes relative to average tumor volumes of methylcellulose group. Right segment: Representative MRI-pictures of respective treatment groups. (e) Phosphorylation status of NDRG1 at T346 24 and 48 h after treatment with the SGK1 inhibitor EMD638683 (left panel) and TMZ-mediated shift of G2/M-phase in U87MG cells treated with EMD638683 relative to DMSO (vehicle) (right panel, $*p < 0.05$ for the effect of LV-*NDRG1*, $^{+}p < 0.05$ for the effect of EMD).

Figure 4: NDRG1 interacts with the DNA repair proteins MGMT, APEX1 and PNKP and promotes MGMT-mediated protection from TMZ

(a) Split Ubiquitin Screen for interaction partners of NDRG1 (NNMT: Nicotinamide N-methyl transferase). (b) Validation of the interaction of NDRG1 with MGMT, PNKP and APEX1 *via* co-immunoprecipitation using HEK293T lysates and Flag-/Myc-tagged constructs of NDRG1, MGMT, PNKP and APEX1, respectively. (c) Cell cycle and proliferation analysis of si*RNA*-

treated U87MG and T98G cells targeting *APEX1* and *PNKP*. Experiments were performed three times with one representative example shown. (d) Cell cycle analysis after si*RNA* mediated knock-down of *MGMT* in T98G cells in response to 300 µM (regular dose) or 20 µM TMZ. (e) Upper panel: BiFC assay with NDRG1. HEK293T cells co-transfected with *NDRG1* in pGW-myc-LC151 and bJun in pGW-HA-LN-151 as negative control (1,3) or with *MGMT* in pGW-HA-LN-151 (2,4). The overlay with the DAPI stain shows a clear nuclear localization of the NDRG1 interaction with MGMT (2,4). Lower panel: PLA with NDRG1 and MGMT. Parental T98G cells exposed to 1% O_2 for 72 h are analysed for interaction of NDRG1 and MGMT (n = 3). Relevant controls are depicted in Fig. S9b. (f) Upper panel: Schematic overview on the location of SGK1-target residues within the C-terminus of the NDRG1 protein. Middle panel: BiFC assay with genetically modified versions of *NDRG1* resulting in amino acid substitutions. HEK293 cells co-transfected with *wt-NDRG1* (left picture), T346V-T356V-*NDRG1* (middle picture) or T328V-S330A-T346V-T356V-*NDRG1* (right picture). Lower panel: Quantification of interaction between MGMT and the three NDRG1-versions depicted as mean fluorescence intensity.

Figure 5: NDRG1 stabilizes MGMT

(a) Time-dependent abundance of MGMT, pNDRG1^{T346} and NDRG1 proteins in T98G cells (Co: control transfected cells; ND: cells lentivirally overexpressing *NDRG1*) after treatment with actinomycin D (upper panel) or TMZ (lower panel). (b) Immunofluorescent staining of O^6-methylguanine of TMZ-treated T98G LV-Co and LV-NDRG1 cells (upper row) and quantification of relative O^6-methylguanine content depicted as log-transformed fluorescence for three independent replications (lower row). (c) Schematic overview of the signaling cascade with iatrogenic and microenvironmental activating factors (left side) as well as options for therapeutic intervention (right side). (d) Progression-free survival of the NOA-08 cohort patients differentiated according to *MGMT* promoter methylation status (methylated, +; unmethylated, -) and steroid use in the temozolomide treatment group.

Figure 1

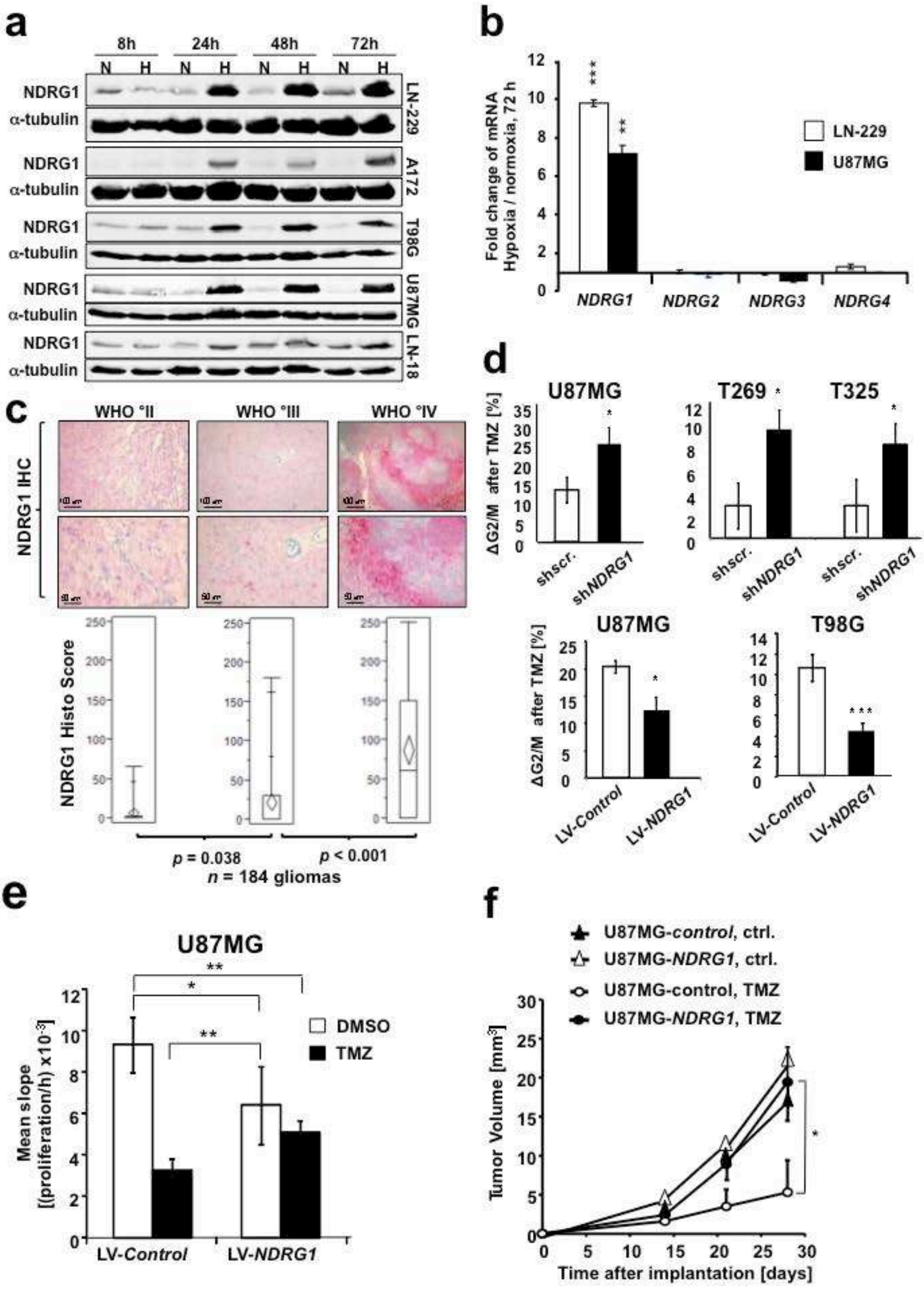
a
8h
24h
48h
72h
N H N H N H N H
NDRG1
α-tubulin
LN-229
A172
T98G
U87MG
LN-18
b
Fold change of mRNA Hypoxia / normoxia, 72 h
LN-229
U87MG
NDRG1
NDRG2
NDRG3
NDRG4
c
WHO °II
WHO °III
WHO °IV
NDRG1 IHC
NDRG1 Histo Score
p = 0.038
p < 0.001
n = 184 gliomas
d
U87MG
T269
T325
ΔG2/M after TMZ [%]
shscr.
shNDRG1
U87MG
T98G
LV-Control
LV-NDRG1
e
U87MG
Mean slope [(proliferation/h) x10-3]
DMSO
TMZ
LV-Control
LV-NDRG1
f
U87MG-control, ctrl.
U87MG-NDRG1, ctrl.
U87MG-control, TMZ
U87MG-NDRG1, TMZ
Tumor Volume [mm3]
Time after implantation [days]

Figure 2

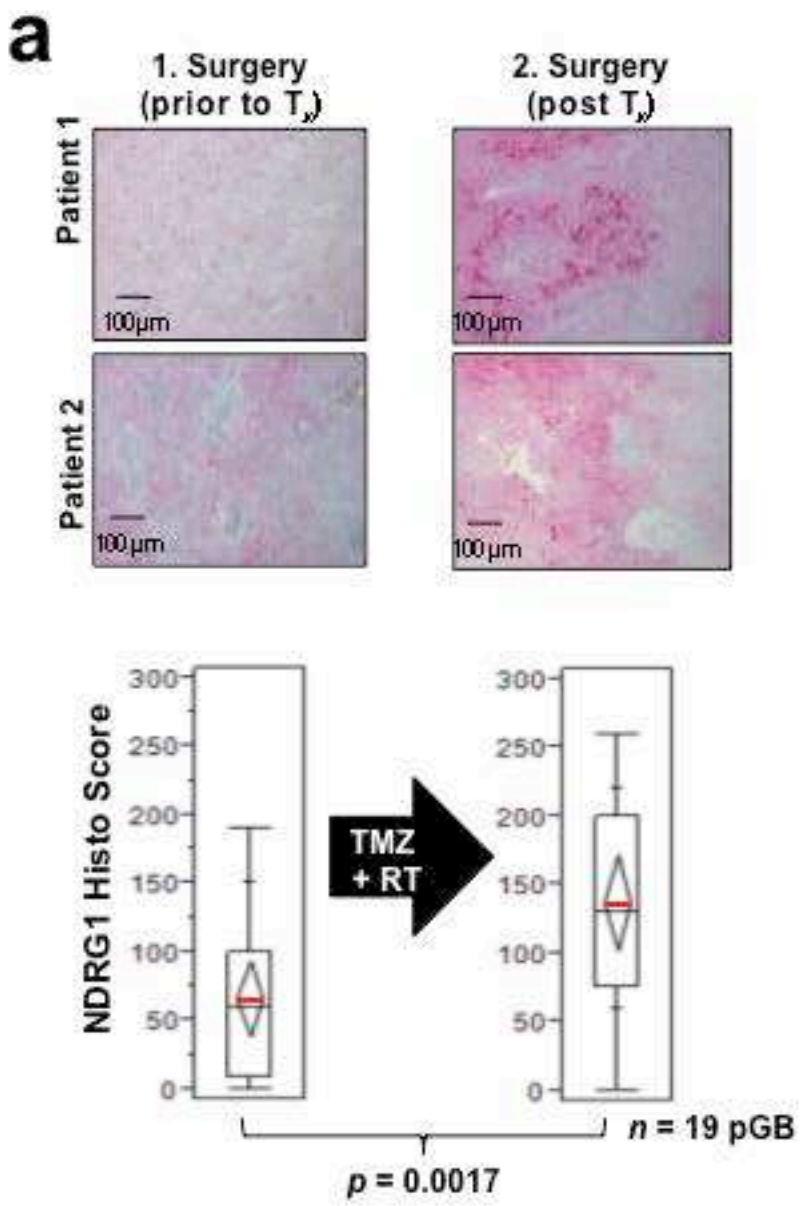

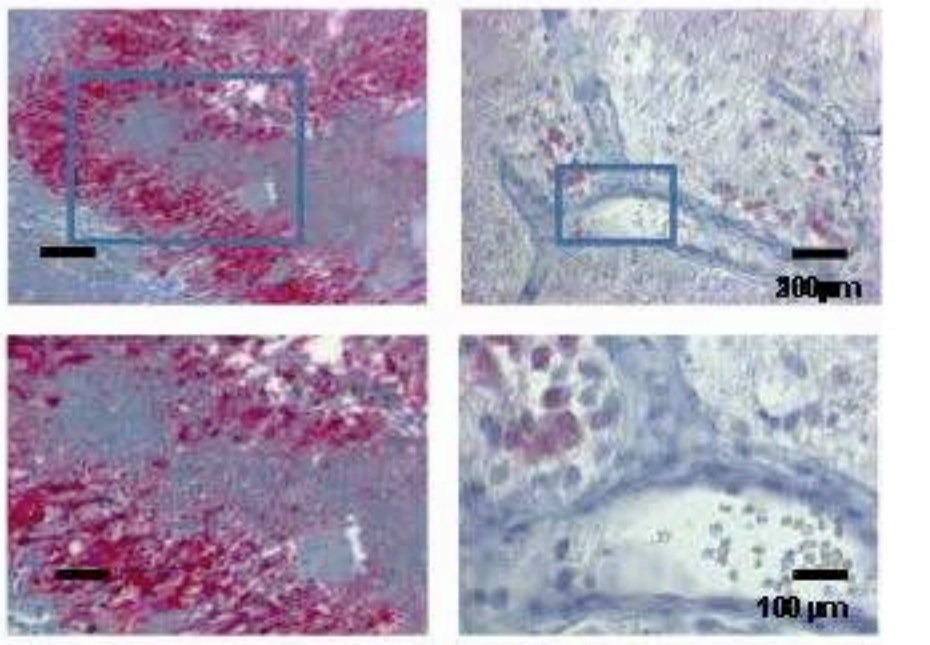

Patient	Pre-therapeutic	Post-therapeutic
1	0/10	8/16
2	0/10	12/20
3	4/18	12/20
4	0/40	0/8
5	0/25	11/12
6	8/20	20/30

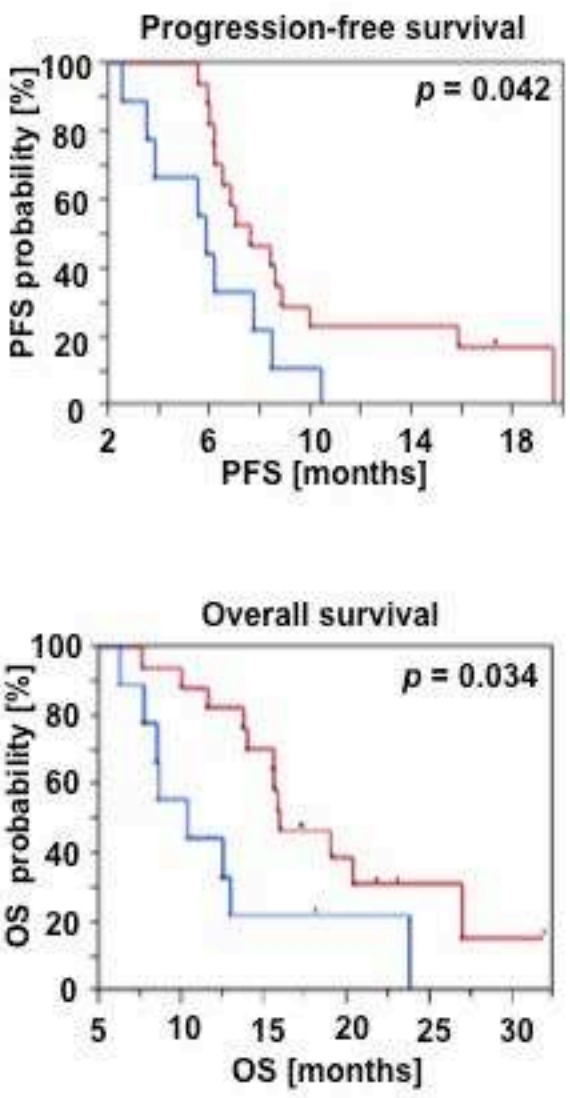

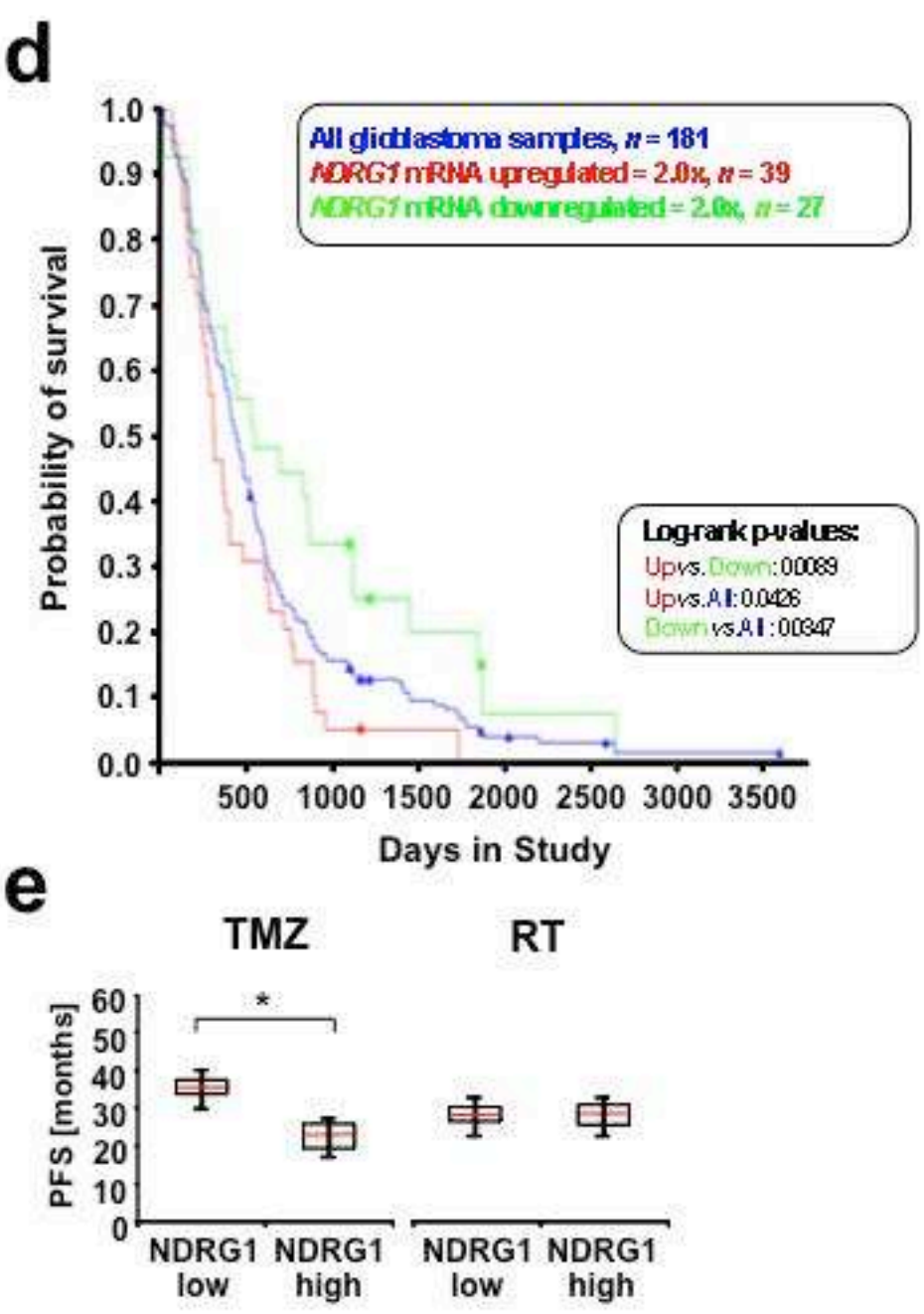

Figure 3

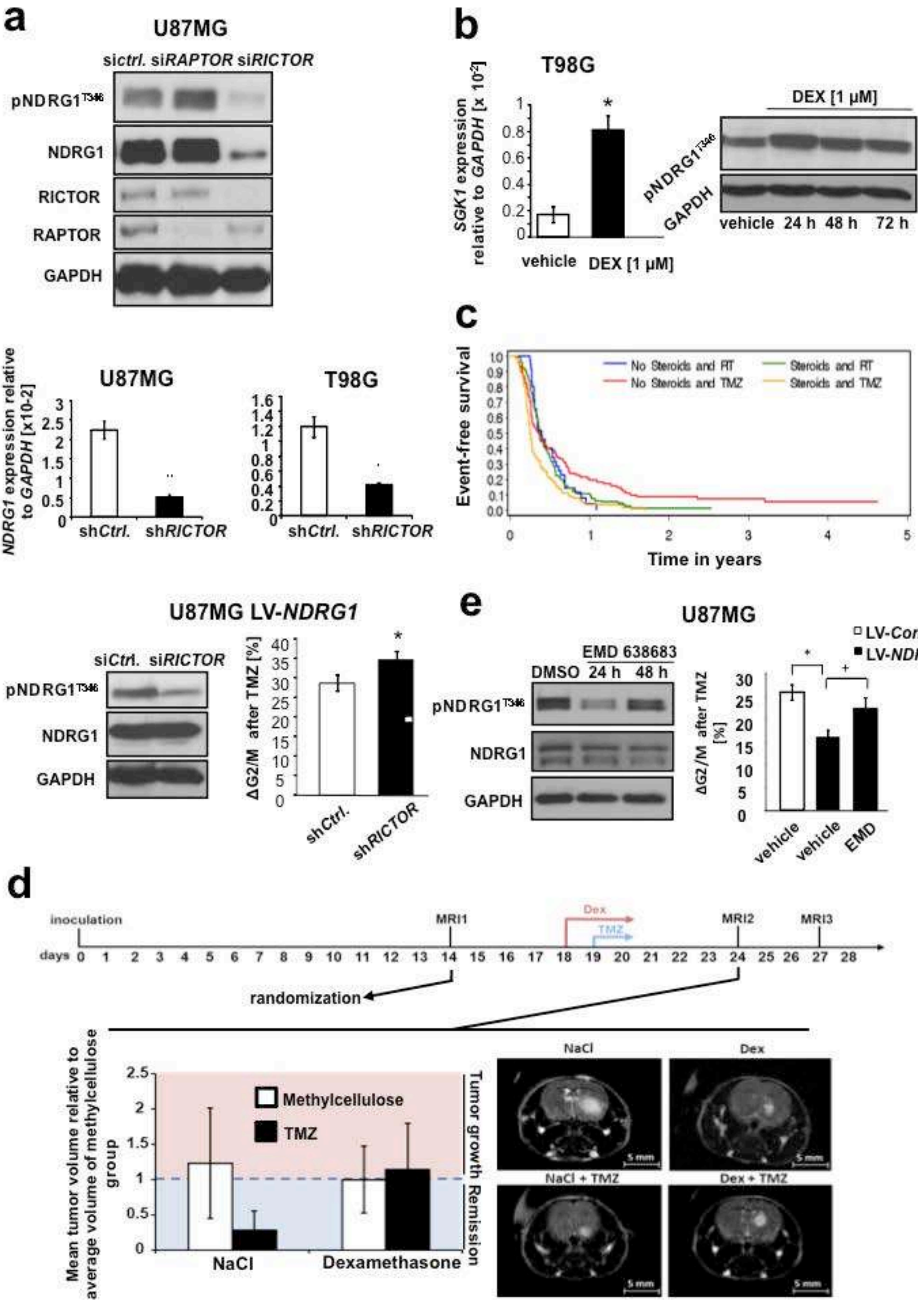
a
U87MG
siCtrl. siRAPTOR siRICTOR
pNDRG1T346
NDRG1
RICTOR
RAPTOR
GAPDH
b
T98G
SGK1 expression relative to GAPDH [x 10-2]
vehicle
DEX [1 µM]
DEX [1 µM]
pNDRG1T346
GAPDH
vehicle 24 h 48 h 72 h
c
Event-free survival
No Steroids and RT
No Steroids and TMZ
Steroids and RT
Steroids and TMZ
Time in years
U87MG
NDRG1 expression relative to GAPDH [x10-2]
shCtrl.
shRICTOR
T98G
shCtrl.
shRICTOR
U87MG LV-NDRG1
siCtrl. siRICTOR
pNDRG1T346
NDRG1
GAPDH
ΔG2/M after TMZ [%]
shCtrl.
shRICTOR
e
U87MG
LV-Control
LV-NDRG1
EMD 638683
DMSO 24 h 48 h
pNDRG1T346
NDRG1
GAPDH
ΔG2/M after TMZ [%]
vehicle
vehicle
EMD
d
inoculation
MRI1
Dex
TMZ
MRI2
MRI3
days 0 1 2 3 4 5 6 7 8 9 10 11 12 13 14 15 16 17 18 19 20 21 22 23 24 25 26 27 28
randomization
Mean tumor volume relative to average volume of methylcellulose group
Methylcellulose
TMZ
NaCl
Dexamethasone
Tumor growth Remission
NaCl
Dex
NaCl + TMZ
Dex + TMZ
5 mm

Figure 4

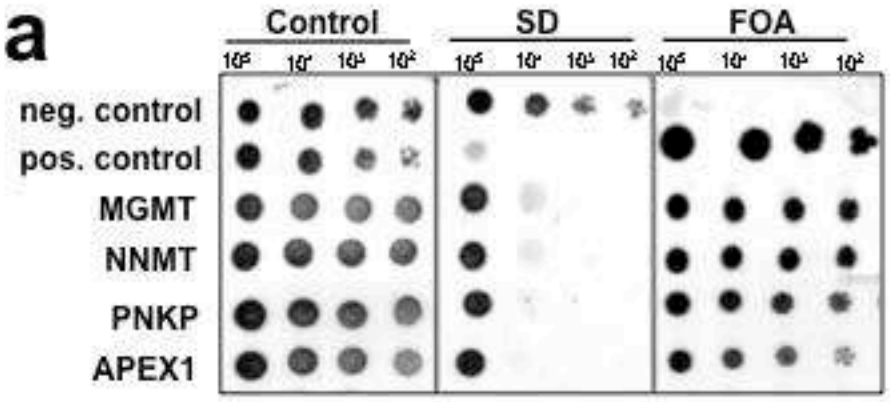
a
Control
SD
FOA
neg. control
pos. control
MGMT
NNMT
PNKP
APEX1

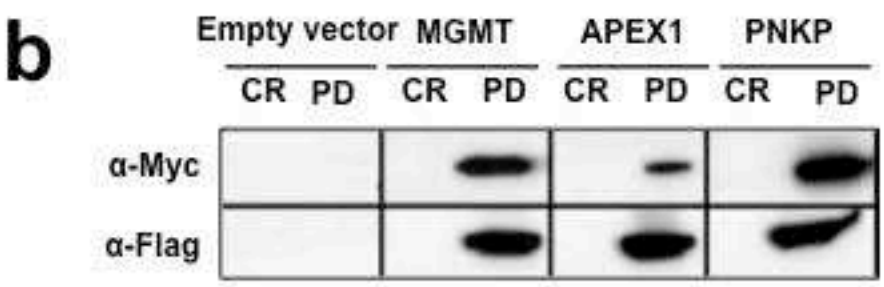
b
Empty vector
MGMT
APEX1
PNKP
CR
PD
α-Myc
α-Flag

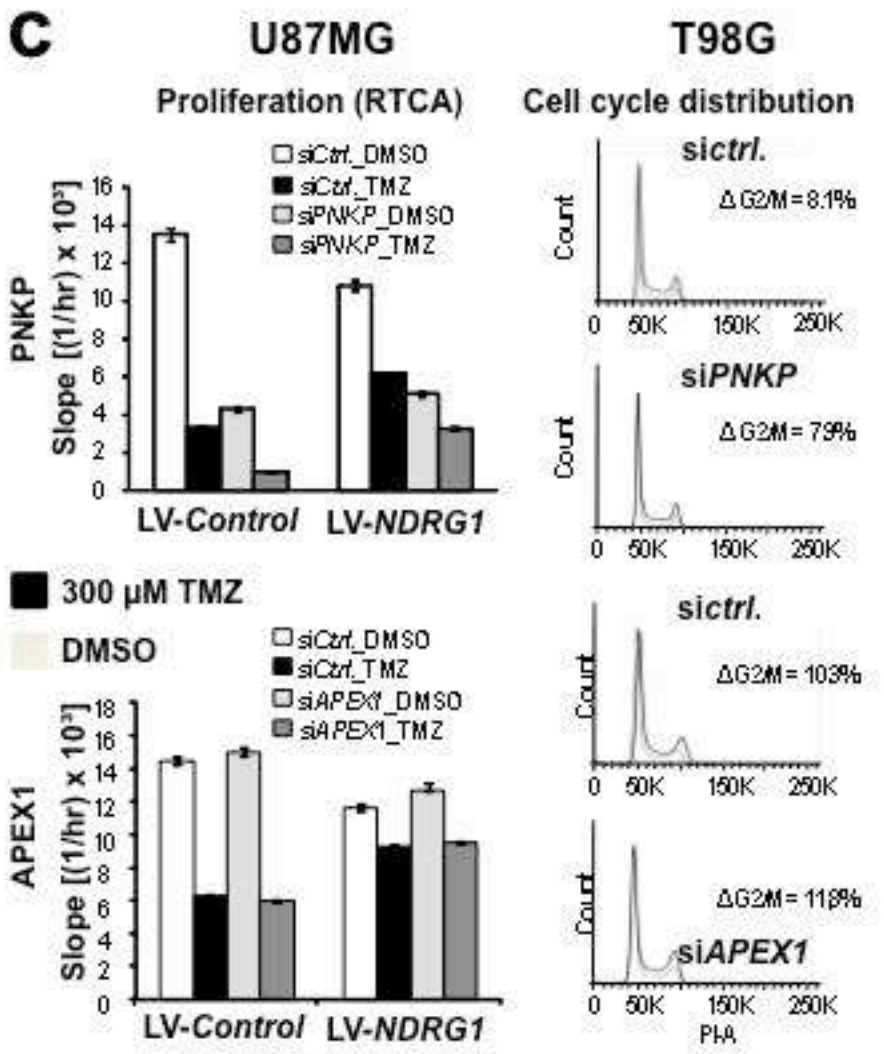
c
U87MG
Proliferation (RTCA)
siCtrl_DMSO
siCtrl_TMZ
siPNKP_DMSO
siPNKP_TMZ
PNKP
Slope [(1/hr) x 10³]
LV-Control
LV-NDRG1
300 µM TMZ
DMSO
siCtrl_DMSO
siCtrl_TMZ
siAPEX1_DMSO
siAPEX1_TMZ
APEX1
Slope [(1/hr) x 10³]
LV-Control
LV-NDRG1
T98G
Cell cycle distribution
sictrl.
ΔG2/M = 8.1%
siPNKP
ΔG2/M = 79%
sictrl.
ΔG2/M = 103%
ΔG2/M = 118%
siAPEX1
Count
PI-A

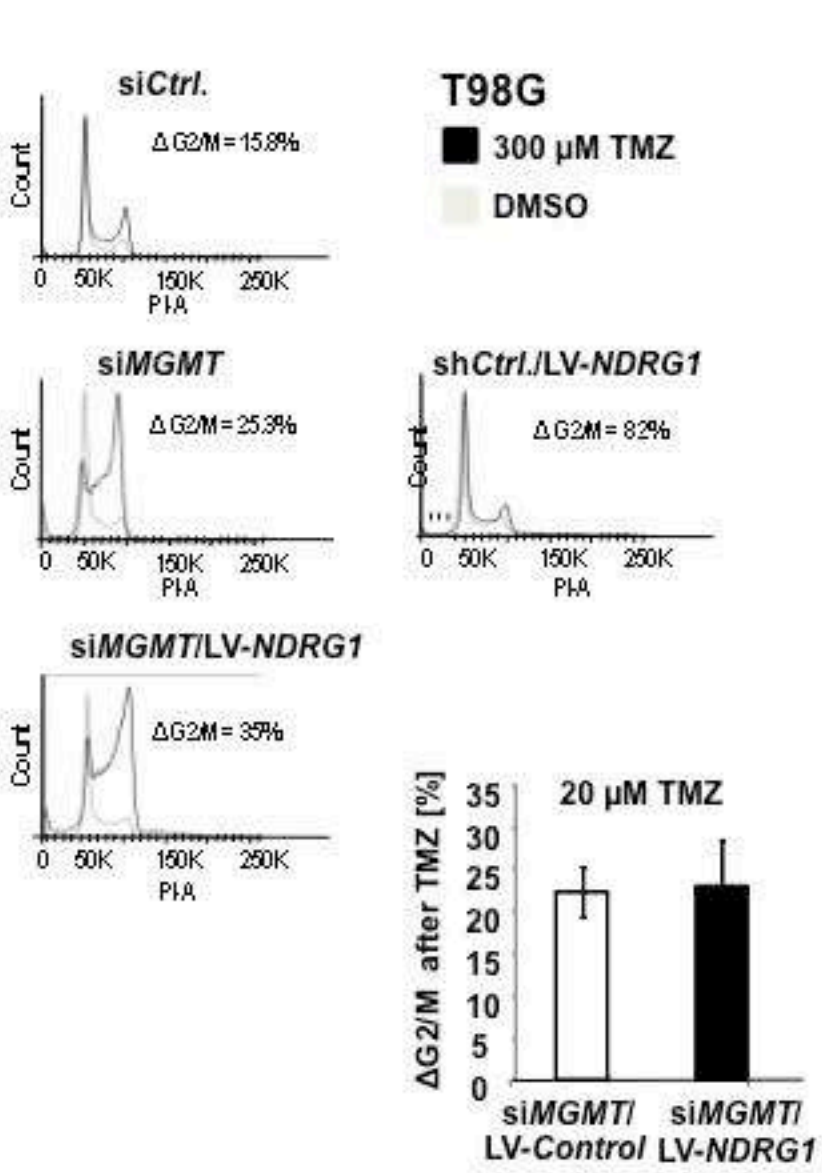
d
siCtrl.
ΔG2/M = 15.8%
T98G
300 µM TMZ
DMSO
siMGMT
ΔG2/M = 25.3%
shCtrl./LV-NDRG1
ΔG2/M = 82%
siMGMT/LV-NDRG1
ΔG2/M = 35%
Count
PI-A
ΔG2/M after TMZ [%]
20 µM TMZ
siMGMT/ LV-Control
siMGMT/ LV-NDRG1

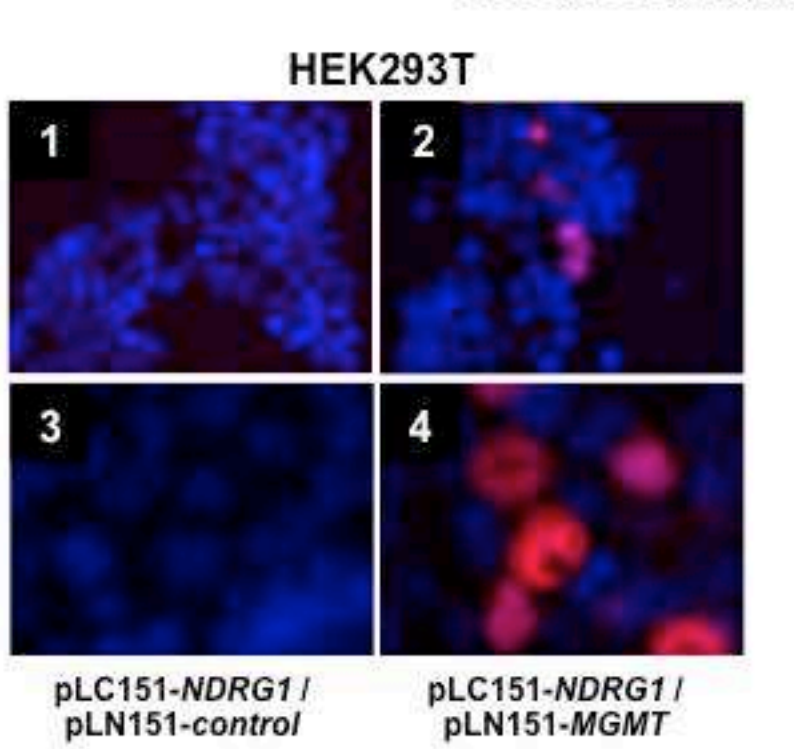
e
HEK293T
1
2
3
4
pLC151-NDRG1 / pLN151-control
pLC151-NDRG1 / pLN151-MGMT
T98G
DAPI
MGMT/NDRG1 red detection
MGMT/NDRG1 merge
NDRG1 only merge

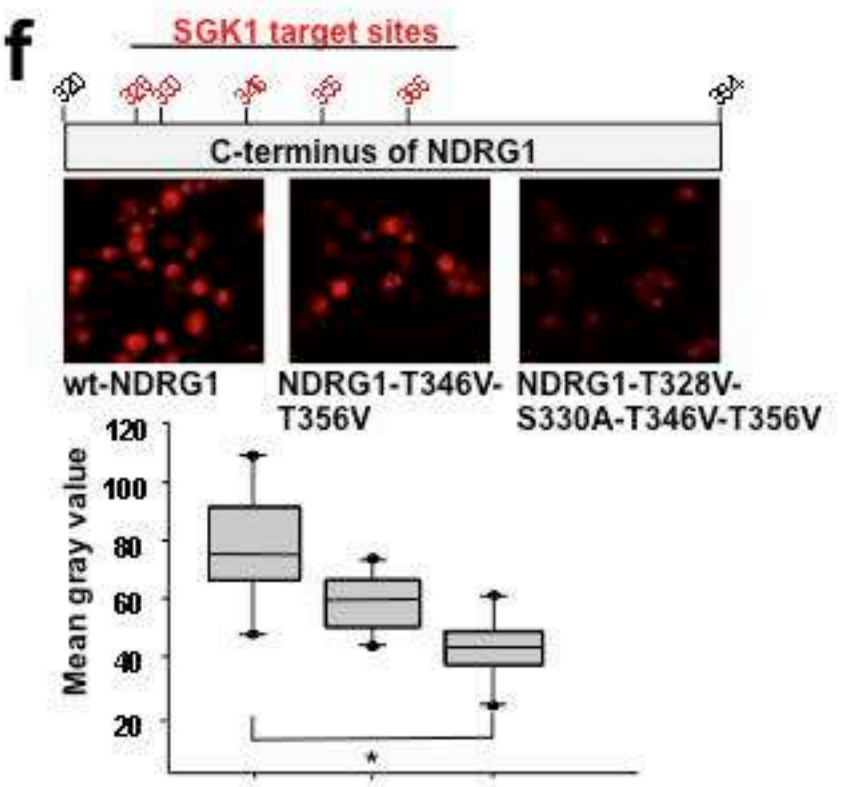
f
SGK1 target sites
C-terminus of NDRG1
wt-NDRG1
NDRG1-T346V-T356V
NDRG1-T328V-S330A-T346V-T356V
Mean gray value
*

Figure 5

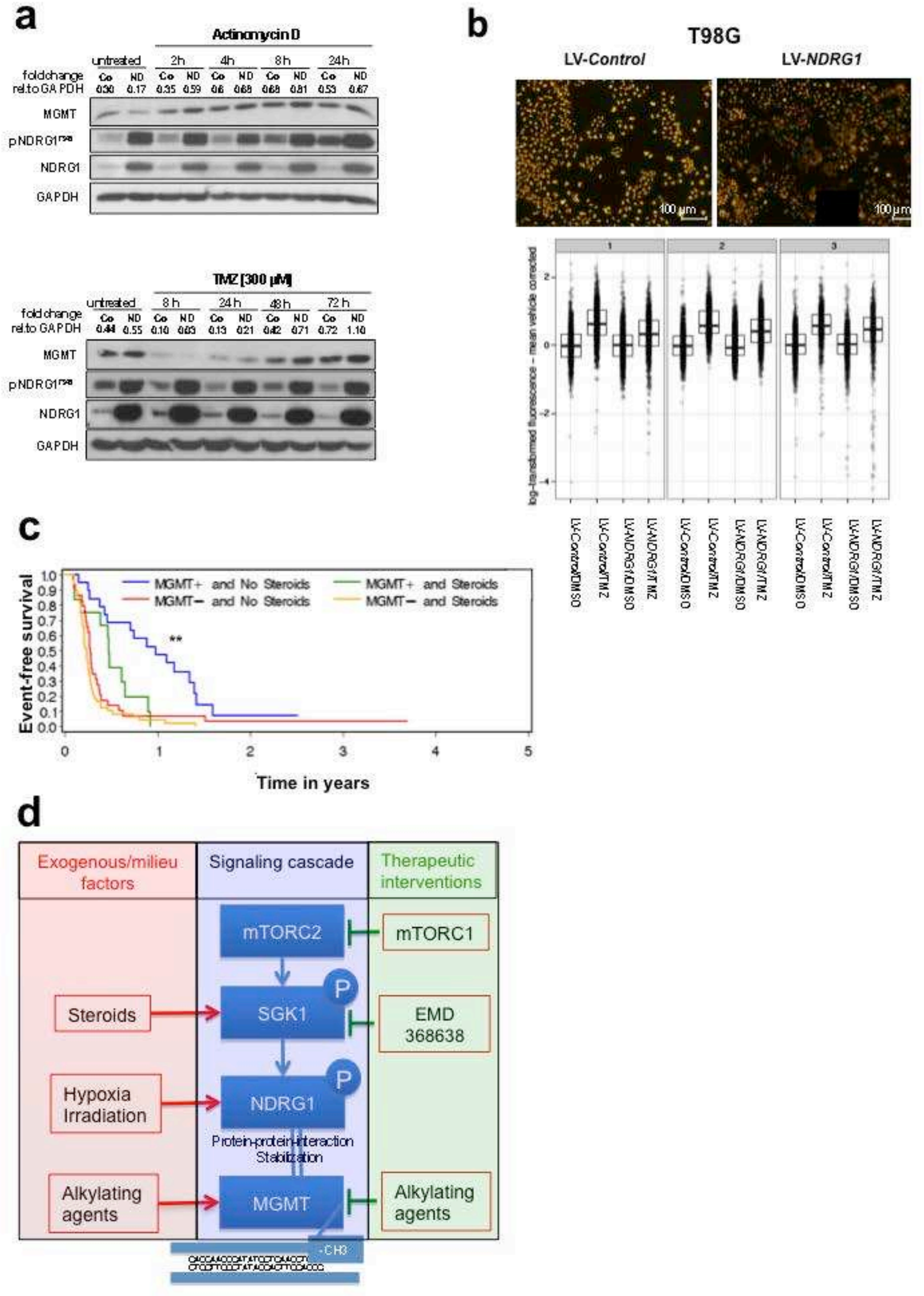
a
Actinomycin D
untreated
2h
4h
8h
24h
fold change rel.to GAPDH
Co ND Co ND Co ND Co ND Co ND
0.30 0.17 0.35 0.59 0.6 0.68 0.68 0.81 0.53 0.67
MGMT
pNDRG1Thr346
NDRG1
GAPDH
TMZ [300 µM]
untreated
8 h
24 h
48 h
72 h
fold change rel.to GAPDH
Co ND Co ND Co ND Co ND Co ND
0.44 0.55 0.10 0.03 0.13 0.21 0.42 0.71 0.72 1.10
MGMT
pNDRG1Thr346
NDRG1
GAPDH
b
T98G
LV-Control
LV-NDRG1
100 µm
100 µm
log-transformed fluorescence - mean vehicle corrected
1
2
3
LV-Control/DMSO
LV-Control/TMZ
LV-NDRG1/DMSO
LV-NDRG1/TMZ
c
Event-free survival
MGMT+ and No Steroids
MGMT− and No Steroids
MGMT+ and Steroids
MGMT− and Steroids
**
Time in years
d
Exogenous/milieu factors
Signaling cascade
Therapeutic interventions
mTORC2
mTORC1
P
SGK1
EMD 368638
Steroids
Hypoxia
Irradiation
NDRG1
Protein-protein-interaction
Stabilization
Alkylating agents
MGMT
Alkylating agents
-CH3